A new method to determine wall shear stress distribution

A new method to determine wall shear stress distribution

F. J. H. Gijsen,[a] A. Goijaerts, F. N. van de Vosse, and J. D. Janssen

Department of Mechanical Engineering, Eindhoven University of Technology, P.O. Box 513, 5600 MB Eindhoven, The Netherlands

(Received 2 December 1996; final version received 2 June 1997)

Synopsis

The absence of a model to predict near wall viscosity of complex suspensions instigated an investigation for a new method to determine the wall shear stress. If the inner wall of a flow model is covered with a highly flexible gel layer, the local wall shear stress will deform this gel layer. Through the known properties of the gel layer, the measured deformation can be transformed to the wall shear stress. To measure the deformation of the gel layer, speckle pattern interferometry was applied. The performance of the developed speckle apparatus was evaluated using a well-controlled benchmark experiment, and a resolution of 50 nm was achieved. The deformation of a gel layer was measured in a two-dimensional rectangular duct, using a Newtonian and a non-Newtonian measuring fluid. The wall shear stresses were measured as a function of the flow rate and compared to theoretical predictions, and the results demonstrated the potential of the method. © *1997 The Society of Rheology.* [S0148-6055(97)01005-5]

I. INTRODUCTION

The wall shear stress, exerted by a fluid flowing over a solid surface, is important to comprehend the performance of various systems. Determination of the wall shear stress can be applied to optimize drag reduction in pipe flow or skin friction in aerodynamics. In a more fundamental application, the wall shear stress measurements can be combined with fluid velocity measurements to evaluate the performance of constitutive models. This paper focuses on a physiological application: the role of wall shear stress in the development of atherosclerosis. Atherosclerosis is a complex disease that causes a progressive occlusion of the arteries. The predilection of atherosclerosis for specific sites in the arterial tree is believed to be related to low or oscillating wall shear stresses [Nerem (1992)]. The wall shear stress is defined as the product of the wall shear rate ($\dot{\gamma}$) and the dynamic viscosity (η). Currently, the wall shear stress in the arterial system is determined from ultrasound velocity measurements: the measured velocity distribution is extrapolated to the wall and the wall shear rate is determined, and a model for the viscosity of blood near the wall is adopted [e.g., Tangelder *et al.* (1986)]. Validation of this clinical procedure to evaluate blood flow induced wall shear stresses in a physiologically relevant flow (e.g., flow over a backwards facing step) is desirable.

The extrapolation of the velocity profile to obtain the wall shear rate can be evaluated by using an alternative method, e.g., hot wire anemometry [Mann and Tarbell (1990)]. A review on other available methods to measure wall shear rate is given by Hanratty and

[a]Address correspondence to F.J.H.Gijsen at W-hoog4.146, Eindhoven University of Technology, P.O. Box 513, 5600 MB Eindhoven, The Netherlands.

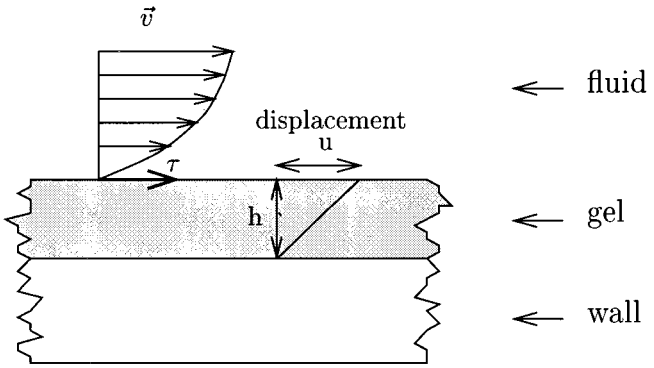

FIG. 1. Wall shear stress measurement through displacement of the gel layer.

Campbell (1983). The estimation of the viscosity of concentrated suspensions, such as blood, at near wall sites poses major difficulties. The constitutive behavior of blood is governed by the suspended particles. Both in viscometric flow and in tube flow, the concentration distribution of the suspended particles in blood is not homogeneous [Goldsmith (1993), Karnis *et al.* (1966)]. Therefore, the viscosity of blood near the wall can not be inferred directly from viscometric experiments. As a consequence, an accurate determination of the wall shear stress, exerted by the flow of a complex suspension such as blood, requires a different measurement technique.

Instead of focusing on the fluid, the response of a sensing element, attached to the wall, can be used to measure the wall shear stress. In aerodynamics, the wall shear stress in air flows is often measured using compact strain gauges that consist of a sensing element that can move parallel to the boundary of the wall. The deformation of the element, or the force required to keep it in its original position, is a measure for the wall shear stress. A review of the available gauges is given by Winter (1977). If the value of the wall shear stress is low, as expected in blood flow [maximum values: 2–3 Pa, Giddens *et al.* (1990)], an accurate measurement of the stress is only possible if the surface of the sensing element is relatively large, thus, limiting the applicability of these devices in physiologically relevant geometries. Tanner and Blows (1976) measured the thickness of an oil film in air flow and related the thickness variation to the wall shear stress distribution. Although the thickness of the oil layer was measured quite accurately, the method was inapt for measuring absolute values of the wall shear stress. Combined with its quasistatic nature, the application of this method is limited. Parmar (1991) investigated the applicability of shear stress sensitive liquid crystals to determine the wall shear stress. When the liquid crystals are illuminated with white light, the reflected light will change color when the crystals are subjected to a mechanical load. Although the response time of the crystals is very short, the resolution of this method (5 Pa) is too low for physiological applications.

In this paper, an alternative method to determine the wall shear stress will be presented (Fig. 1). A highly deformable gel layer is used as the sensing element. The gel layer is attached to the inner wall of a flow model. The wall shear stress, exerted by the fluid, deforms the gel layer slightly. The small deformation of the gel layer can be measured accurately by means of speckle pattern interferometry (SPI). Through the known properties of the gel, the wall shear stress can be inferred from the deformation of the gel layer:

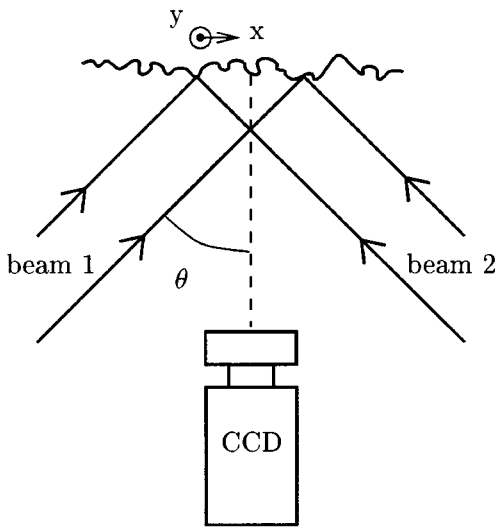

FIG. 2. In-plane displacement measurement with SPI.

$$\tau = \eta \cdot \dot{\gamma} = G \cdot \left(\frac{du}{dh} \right) \approx \frac{G}{h} \cdot u, \tag{1}$$

where G is the shear modulus, h the thickness, and u the displacement of the gel layer. Using this method, the wall shear stress can be determined without prior knowledge of the viscosity of the fluid. In this paper, it will be shown that the proposed method can be used to determine physiologically relevant wall shear stress values. This will be demonstrated by measurement of the wall shear stress in a rectangular duct under steady flow conditions, using water as a measuring fluid. The experimental data are compared to the analytically determined wall shear stress values. It will be shown that the method can also be applied to measure the influence of bloodlike shear thinning behavior on the wall shear stress. The results for the shear thinning non-Newtonian fluid are compared to numerically determined values, using a generalized Newtonian model. If blood is used as a measuring fluid, the combination of the proposed method and clinically applied velocity measurements in a physiologically relevant geometry can be used to validate the procedure to determine wall shear stresses in arteries.

II. EXPERIMENTAL METHODS

The feasibility of the proposed method is assessed by measuring the wall shear stress in a rectangular duct. The deformation of the gel layer, attached to the inner wall of the duct is measured by means of speckle pattern interferometry. The principle of SPI used in this study will be explained briefly, followed by a description of the SPI apparatus, the setup, and the experimental fluids.

A. Speckle pattern interferometry

When a monochromatic light source illuminates a diffusive surface, the reflected light interferes and a speckle pattern is generated. In the configuration of Fig. 2, two laser beams are used to illuminate the diffusive surface, and the speckle pattern is recorded by a CCD camera. The speckle pattern can be used to measure displacements of the surface in the plane of the laser beams, perpendicular to the viewing direction of the camera

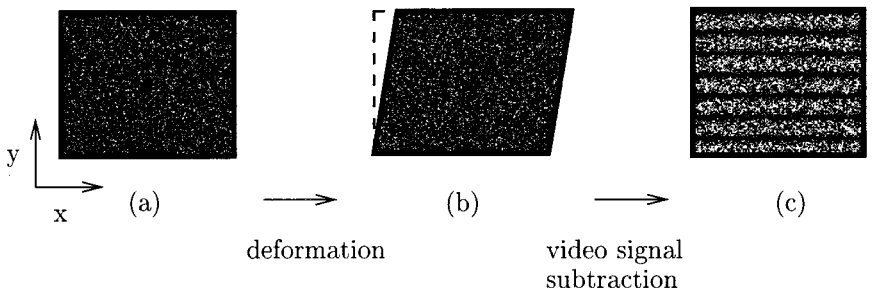

FIG. 3. In-plane displacement measurement on a surface subjected to shear: image of the undeformed surface (a), the deformed surface (b), and the fringe pattern after video signal subtraction (c).

[Jones and Wykes (1989)]. The two laser beams each generate a speckle pattern, and the two speckle patterns interfere. The intensity distribution on the image plane of the CCD camera $I(x,y)$, can be decomposed into the intensities of the two separate speckle patterns and an interference term,

$$I(x,y) = I_1(x,y)+I_2(x,y)+2\sqrt{I_1(x,y)I_2(x,y)}\,\cos[\phi(x,y)], \tag{2}$$

where (x,y) denotes the position vector on the image plane of the CCD, $I_1(x,y)$ and $I_2(x,y)$ the intensities of laser beam 1 and 2, respectively, and the third term is the interference term. The contribution of the interference term depends on the phase difference $[\phi(x,y)]$ between the two laser beams. The phase difference between the two laser beams depends on the surface height, leading to a random distribution of the intensity. If the surface is subjected to small deformations (deformation in the order of the wavelength of the laser light), I_1 and I_2 remain unchanged while the phase difference between the two laser beams reflected from the diffusive surface changes $[\phi(x,y)+\delta(x,y)]$, and so will the contribution of the interference term. The simplest way of obtaining information of the displacement induced phase difference $\delta(x,y)$ is the application of video signal subtraction. If the intensity of the recorded speckle pattern before deformation is subtracted from the intensity of the speckle pattern after deformation of the surface, the resulting intensity distribution (I_r) is

$$I_r(x,y) = 4\sqrt{I_1(x,y)I_2(x,y)}\left|\sin\tfrac{1}{2}[\phi(x,y)+\delta(x,y)]\sin\tfrac{1}{2}[\delta(x,y)]\right|. \tag{3}$$

The intensity distribution after video signal subtraction still has a random character, but it is modulated by the displacement induced phase difference. The phase difference depends on the in-plane displacement u of the surface and on the configuration of the speckle apparatus

$$\delta(x,y) = \frac{4\pi\sin(\theta)u}{\lambda}, \tag{4}$$

where λ is the wavelength of the laser beam and θ the angle between the laser beam and the viewing direction of the CCD camera (see, also, Fig. 2). The phase change will only occur due to a displacement in the plane of the laser beams, perpendicular to the viewing direction (x direction in Fig. 2). Only one component of the displacement field of the surface can be monitored, and the displacement measurements are not disturbed by the out-of-plane movements.

In Fig. 3, the principle of SPI is demonstrated for a surface subjected to in-plane

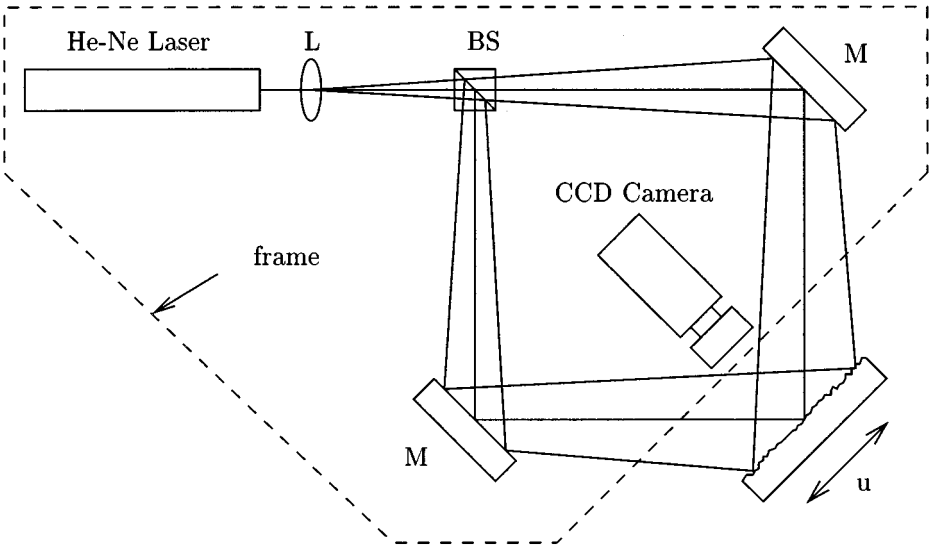

FIG. 4. SPI apparatus.

simple shear. The speckle pattern of the undeformed surface is shown in Fig. 3(a). The deformation of the surface results in a displacement $u(y)$ [Fig. 3(b)]. Since the displacement is a function of y only, the displacement induced phase difference between the laser beams will be a function of y as well [Eq. (4)]. After video signal subtraction, the phase difference δ appears as the argument in the absolute sine function for the resulting intensity [Eq. (3)]. Each time the phase difference is $n \cdot 2\pi$, the resulting intensity shows a local minimum, resulting in a fringe pattern [Fig. 3(c)].

For further reading on SPI, one is referred to Jones and Wykes (1989) and Cloud (1995).

B. Experimental setup

The SPI configuration is schematically shown in Fig. 4. A 10 mW He–Ne laser (105-L, Spectra Physics) produces a laser beam with a diameter of approximately 1 mm and a wavelength of 632.8 nm. The laser beam is expanded by the lens L and split by the beam splitter BS. The two laser beams, reflected by the adjustable mirrors M, eventually overlap on the surface of which the displacement u has to be measured. The CCD camera (MXR, HCS) records the generated speckle patterns. The camera is connected to a PC with a frame grabber. Image processing software (TIM, Difa Measuring Systems) provides the necessary tools for the video signal subtraction. The position of individual components of the apparatus can be adjusted so the angle θ can be varied from 30° to 60° and the dimension of the investigated area from 2×2 mm to approximately 40×40 mm. The performance of the speckle apparatus was evaluated in a benchmark experiment. The displacement of the surface subjected to a small rotation was measured, and repeatability and resolution of 50 nm was achieved.

The deformation of the gel layer was measured in a Plexiglas rectangular duct (height $\times$ width $\times$ length $= 5\times100\times500$ mm). Two constant head tanks provided a constant pressure gradient over the flow model, thus, ensuring steady flow conditions in the setup. The flow rate through the duct was adjusted by controlling the pressure gradient and was monitored by a flow meter (Transflow 601, Skalar) in the outlet tube. The gel layer

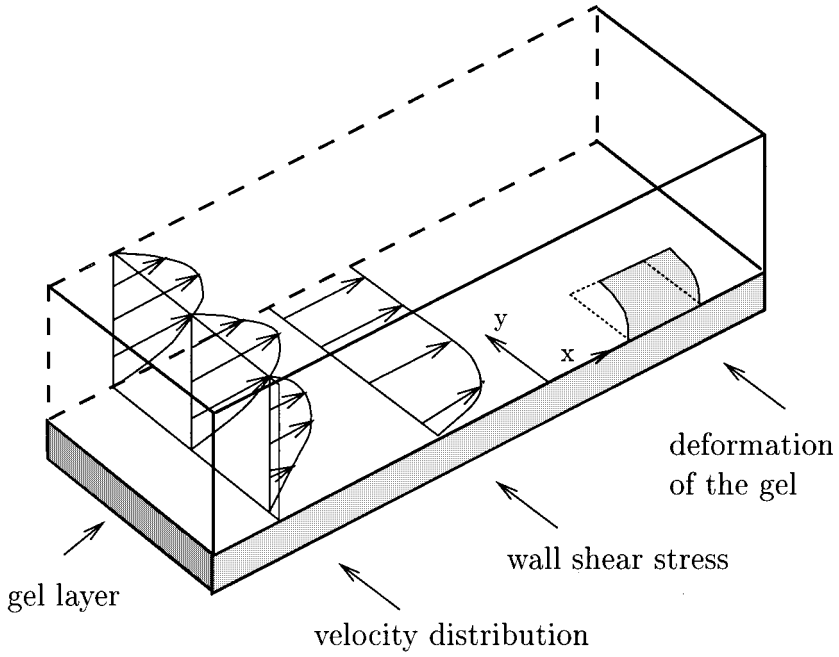

FIG. 5. Schematic presentation of the duct and the expected velocity, shear stress, and deformation distribution.

(height $h = 2.2$ mm) was attached to the lower wall of the duct. Since a diffusive surface is required to perform SPI, a thin layer of titanium oxide (Iriodine 111, Merck) was used to cover part of the gel layer, 350 mm downstream of the entrance of the duct (Fig. 5). The diffusive patch extended from the sidewall ($y = 0$ mm) into the duct ($y = 15$ mm). The deformation of the diffusive patch was measured to determine the wall shear stress. In Fig. 5, the expected wall shear stress distribution in the rectangular duct is shown. In a fully developed flow, the wall shear stress is independent of the axial position and increases from zero at the sidewall to its maximum value in the central part of the duct.

Accurate determination of the wall shear stress from the displacement measurements of the gel depends on a detailed knowledge on the properties of the gel layer [Eq. (1)]. The gel layer was produced from a 3.5% gelatin solution in water, and its properties were measured in a parallel–plate viscometer (Rheometrics, RFSII). Dynamic strain experiments were performed with a strain amplitude of 1% at a frequency of 1 Hz, and the results indicate that the gel was essentially elastic ($G = 600$ Pa). No further treatment of the gelatin or the Plexiglas was required to ensure a proper attachment of the gelatin to the wall of the duct. The height of the gel layer was determined by carefully controlling the amount of the gelatin solution, poured into the duct. During the curing of the gel layer, no change of volume was seen.

C. Experimental fluids

Two fluids were used in this study: a Newtonian fluid to evaluate the performance of the developed method and a non-Newtonian fluid to investigate the influence of shear thinning properties of blood on the magnitude of the wall shear stresses. Water was used as the Newtonian fluid and a Xanthan gum solution (275 ppm in water) served as the non-Newtonian fluid. The steady shear viscosity of the Xanthan gum solution (Fig. 6)

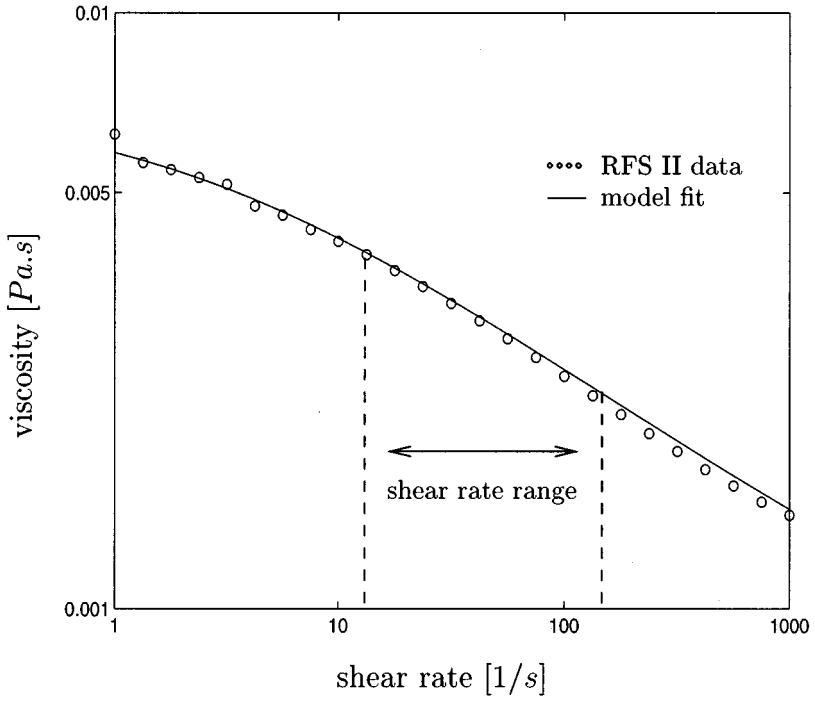

FIG. 6. Measured steady shear viscosity of the Xanthan gum solution (○) and the Carreau–Yassuda fit (—). The shear rate range in the experiments is indicated.

was measured in a parallel–plate viscometer (Rheometrics, RFSII). The Xanthan gum solution mimics the shear thinning behavior of blood as was shown by, e.g., Mann and Tarbell (1990).

To validate the method, the measured wall shear stress was compared to analytically (water) and numerically (Xanthan gum solution) obtained wall shear stress values. From the analytical solution of the velocity field in a rectangular duct [Ward-Smith (1980)], the velocity gradient along the gel layer was computed for the flow rates used in the experiments. The wall shear rates, multiplied by the dynamic viscosity of water, yielded the analytical wall shear stresses, which were compared to the experimental results. The shear thinning behavior of the non-Newtonian fluid was fitted with the Carreau–Yassuda model [Bird *et al.* (1987)]. Using the parameters of this generalized Newtonian model, the velocity distribution, the wall shear rates, and the wall shear stresses were computed with the finite element package SEPRAN [Segal (1992)]. The measured wall shear stresses for the non-Newtonian fluid were compared to the computational results.

III. RESULTS

For the Newtonian fluid, the deformation of the gel layer was measured for seven different flow rates. For each flow rate, the measured speckle pattern was subtracted from the reference speckle pattern at zero flow. Since the flow was assumed to be fully developed and the gel layer to be homogeneous, the displacement of the gel layer was expected to be constant for constant y (see, also, Fig. 5). The fringe distribution should, therefore, exhibit fringes parallel to the side wall of the duct (Fig. 7). The intensity of the measured fringe pattern was averaged over an area Δx, and the resulting fringe distribu-

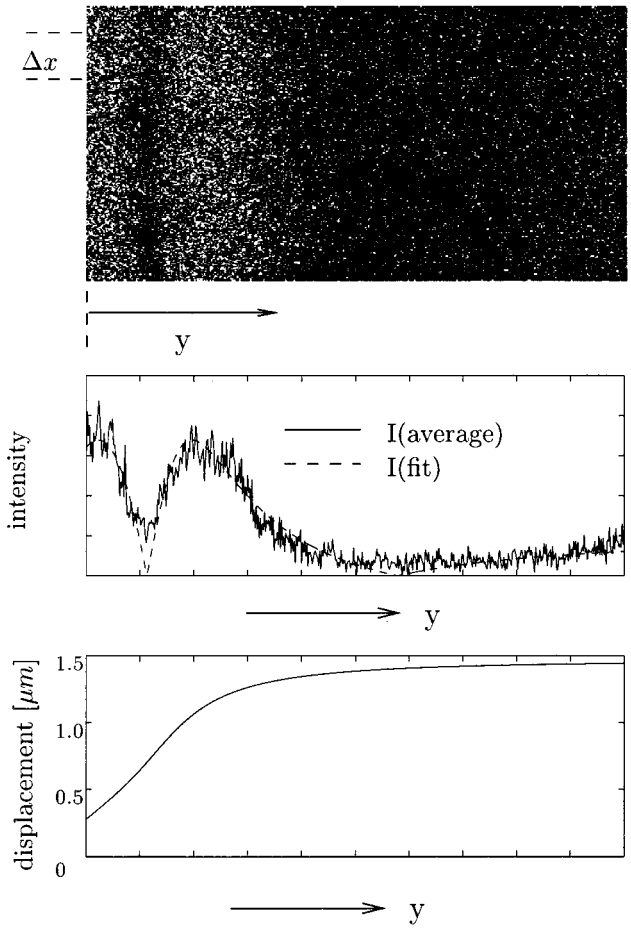

FIG. 7. Fringe distribution (top) at a flow rate of 1.11 l/min, the averaged and fitted irradiance distribution (center), and the resulting displacement (bottom).

tion was approximated by an absolute sine function [Eq. (3)]. The approximation procedure resulted in an optimal fitted intensity distribution that was converted to a displacement through Eq. (4).

The procedure is visualized in Fig. 7 for a flow rate of 1.11 l/min. On the top, the measured fringe pattern is depicted. The averaged and fitted mean intensity are shown in the center, and the resulting displacement on the bottom part. The expected fringe pattern, with the fringes parallel to the wall, can be discerned clearly. In the averaged fringe distribution, the position of the fringes can be seen readily. The fitting procedure yields a displacement distribution that is nonzero at the wall: this is caused by a displacement of the duct. This off-set of the displacement can be subtracted from the fitted displacement to obtain the displacement of the gel layer.

The measured wall shear stress was inferred directly from the displacement through Eq. (1) and compared to the analytical wall shear stress distribution for three flow rates (Fig. 8). In the region that is not affected by the presence of the sidewall, the measured values of the wall shear stress show an excellent agreement with the analytical wall shear stress values. Near the sidewall, the measured wall shear stress is substantially lower than the analytical wall shear stress. This can be attributed to the kinematic boundary condi-

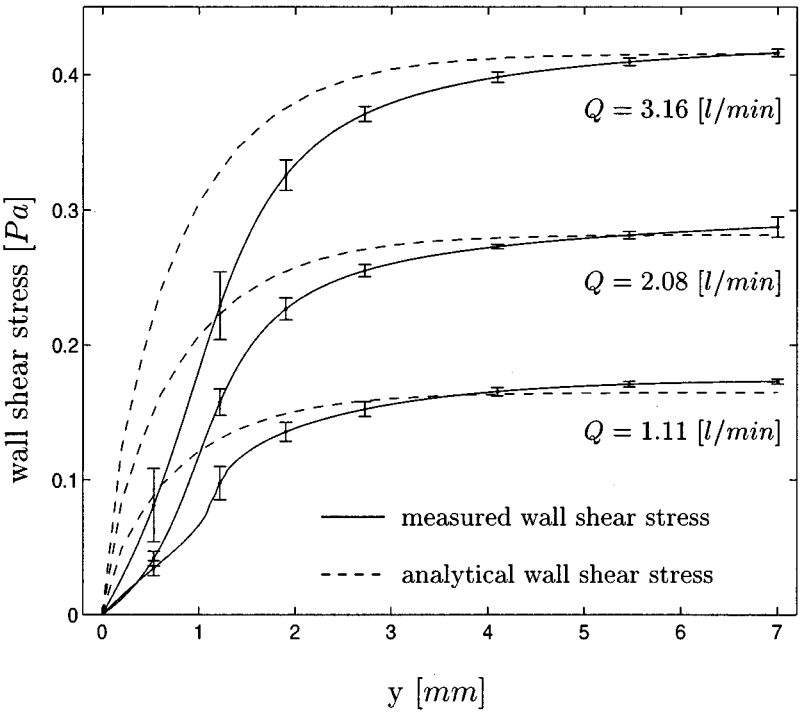

FIG. 8. Wall shear stress as a function of the distance from the sidewall (y). A comparison between the measured and the analytical wall shear stresses for three different flow rates.

tions for the gel layer. The gel layer is not only attached to the bottom wall but also to the sidewall: the displacement of the gel layer close to the sidewall will be lower than one would expect on the basis of Eq. (1).

Finally, a comparison between the analytical and the measured wall shear stress at $y = 7$ mm is presented in Fig. 9. The measured wall shear stress shows an almost perfect linear fit (not shown), but the slope of the fitted line is not exactly equal to 1, being 4% higher. This indicates that the estimated value of G/h is too high: either the thickness of the gel layer or the shear modulus of the gel were not determined accurately, or altered during the measurements.

For the non-Newtonian fluid, the wall shear stress was determined for ten flow rates, ranging from 0.1 to 1.0 l/min. The shear rate varied from 13 to 130 1/s (Fig. 6). As a calibration, the gel layer displacements were also measured using water at flow rates of 0.5 and 1.0 l/min. These measurements were used to determine the value for G/h. This value was used to convert the measured displacement to the wall shear stress for the non-Newtonian fluid. The measured wall shear stress values for the Xanthan gum solution, scaled with the computed values for water, are shown in Fig. 10. As expected for a shear thinning fluid, the wall shear stresses for the Xanthan gum solution decrease as the flow rate increases, and they compare well to the computed values. Only at lower flow rates, some differences can be seen between the measured and the computed values. These discrepancies can be attributed to the increased sensitivity to the inaccuracy in determining the flow rate and counting the fringes.

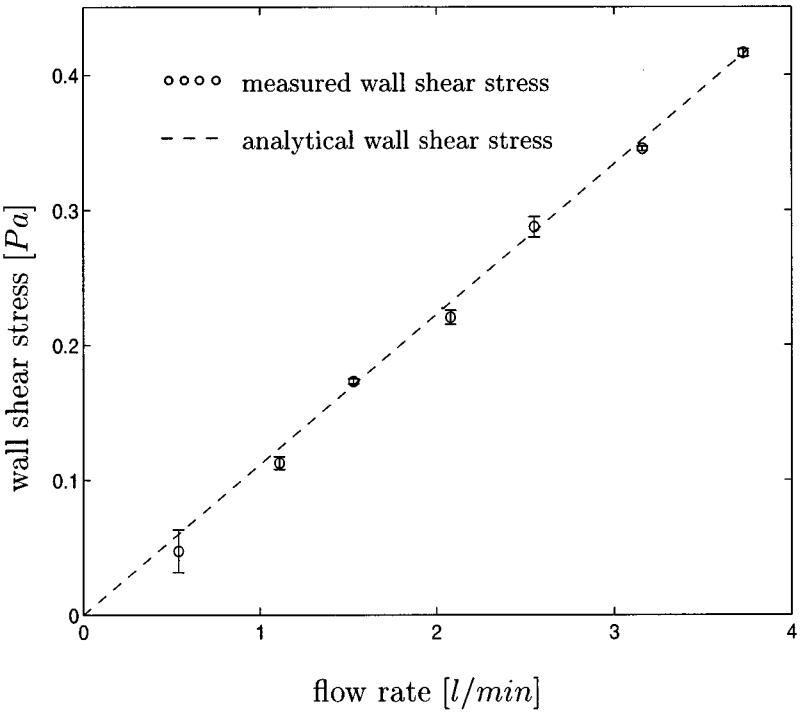

FIG. 9. Measured (○) and analytical (—) wall shear stress as a function of the flow rate at $y = 7$ mm.

IV. DISCUSSION AND CONCLUSIONS

A method to determine the wall shear stress for flow in a rectangular duct was evaluated for a Newtonian and a non-Newtonian fluid. The value of the wall shear stress was inferred from the deformation of an elastic gel layer inside the flow model. The deformation of the gel layer was accurately measured by means of SPI, and through the properties of the gel layer, the wall shear stress was computed. The measured wall shear stress far enough from the sidewall showed a good agreement with the computed wall shear stress for both the Newtonian and the non-Newtonian fluid. The wall shear stress measurements were accurate enough to discriminate between the two fluids. The kinematic boundary conditions for the gel layer influenced its response near the sidewall of the duct. With the proposed method, the wall shear stress can be determined without prior knowledge of the properties of the fluid.

Three aspects determine the accuracy of the wall shear stress measurement: the displacment measurement, the properties of the gel layer, and the loading condition of the gel layer in the flow cell. The displacement measurements were performed with a relatively cheap and simple SPI apparatus. The repeatability and resolution of the SPI apparatus are satisfactory. The main drawback of the apparatus is its lack of directional sensitivity: a positive displacement yields the same fringe pattern as a negative displacement. The properties of the gel layer, the shear modulus of the gel, and the thickness of the layer, transfer the measured displacement to the wall shear stress. Both must be determined accurately and remain unaltered once placed in the flow model. Depending on the chemical composition of the fluid, the gel layer may swell or part of the solid fraction of the gel may dissolve in the fluid. The deviation of the fitted line in Fig. 9 can be attributed to the altered properties of the gel. The application of the method in more

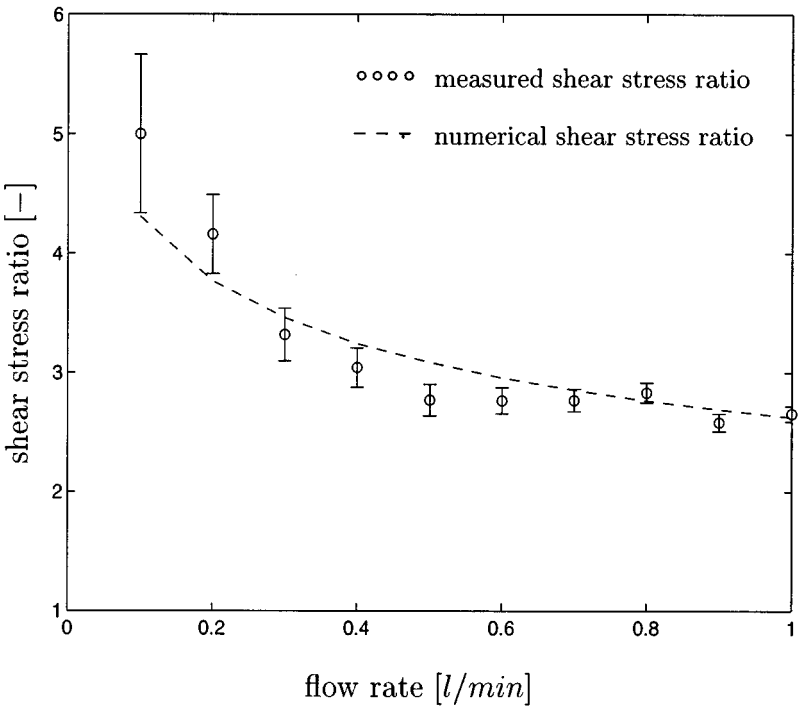

FIG. 10. Scaled measured wall shear stress for the Xanthan gum solution (○), compared to the numerical results (- -) as a function of the flow rate at $y = 7$ mm.

complex flows or fluids should, therefore, be accompanied by a calibration procedure to determine the value of G/h *in situ,* as was done for the non-Newtonian fluid. The third aspect that influences the measured displacement is the loading condition of the gel layer. Equation (1) is only valid for a freely moving gel layer subjected to a shear load. Both the dynamic and the kinematic boundary conditions for the gel layer can alter the response of the gel layer, and Eq. (1) should be regarded with caution. A gradient in the wall shear stress, e.g., in the neighborhood of a stagnation point, results in a load on the gel layer that consists of both shear and tensile stress: Eq. (1) cannot be applied. Equally important for the response of the gel layer are the kinematic boundary conditions, as can be concluded from Fig. 8. The gel layer clings to the sidewall and the response of the gel layer is altered. Extension of this method to physiological flow conditions imposes several additional requirements. Since the displacement of the gel layer in a more complex flow can be both positive and negative, the directional sensitivity of the SPI apparatus is required. Several methods to include directional sensitivity are available [Creath (1985)]. These methods (e.g., phase stepping speckle interferometry) can be used to determine the exact value of the displacement induced phase difference: directional sensitivity is included and the accuracy will improve. A second, and more important requirement, is additional knowledge of the behavior of the gel layer. In a more complex flow, both the wall shear stress gradients and kinematic boundary conditions for the gel layer will influence the response of the gel layer. Since the displacements of the gel layer are small and the gel is elastic, the measured displacements of the gel can be used as a boundary condition for a simple, linear elastic finite element computation to predict the behavior of the gel. The wall shear stress can then be obtained as a result of these computations. The

combination of phase stepping speckle interferometry and a finite element analysis of the gel layer will enable a validation of the *in vivo* procedure to determine the wall shear stress in physiologically relevant flows.

References

Bird, R., R. Armstrong, and O. Hassager, *Dynamics of Polymer Liquids* (Wiley, New York, 1987).

Cloud, G., *Optical Methods of Engineering Analysis* (Cambridge University Press, 1995).

Creath, K., ''Phase-shifting speckle interferometry,'' Appl. Opt. **24**, 3053–3058 (1985).

Giddens, G., C. Zarins, and S. Glagov, ''Response of arteries to near-wall fluid dynamic behavior,'' Appl. Mech. Rev. **43**, S98–S102 (1990).

Goldsmith, H., ''Poiseuille medal award lecture: From papermaking fibers to human blood cells,'' Biorheology **30**, 165–190 (1993).

Hanratty, T. and J. Campbell, ''Measurement of wall shear stress,'' in *Fluid Mechanics Measurements*, edited by R. Goldstein (Hemisphere Publishing, New York, 1983), Chap. 11.

Jones, R. and C. Wykes, *Holographic and Speckle Interferometry* (Cambridge University Press, 1989).

Karnis, A., H. Goldsmith, and S. Mason, ''The kinetics of flowing dispersions. I: concentrated suspensions of rigid particles,'' J. Colloid Interface Sci. **22**, 531–553 (1966).

Mann, D. and J. Tarbell, ''Flow of non-Newtonian blood analog fluids in rigid curved and straight artery models,'' Biorheology **27**, 711–733 (1990).

Nerem, R., ''Vascular fluid mechanics, the arterial wall, and atherosclerosis,'' J. Biomech. Eng. **114**, 274–282 (1992).

Parmar, D., ''A novel technique for response function determination of shear sensitive cholesteric crystals for boundary layer investigations,'' Rev. Sci. Instrum. **62**, 1596–1608 (1991).

Segal, G., Manual SEPRAN package (1992).

Tangelder, G., D. Slaaf, A. Muijtjens, T. Arts, M. oude Egbrink, and R. Reneman, ''Velocity profiles of blood platelets and red blood cells flowing in arterioles of the rabbit mesentry,'' Circ. Res. **59**, 505–514 (1986).

Tanner, L. and L. Blows, ''A study of the motion of oil films on surfaces in air flow, with application to the measurement of skin friction,'' J. Phys. E. **9**, 194–202 (1976).

Ward-Smith, A., *Internal Fluid Flow* (Clarendon, Oxford, 1980).

Winter, K., ''An outline of the techniques available for the measurement of skin friction,'' Prog. Aerospace Sci. **18**, 1–57 (1977).